Radiative lifetimes of $6snsnbsp\ ^3S_1$ and $6snd\ ^3D_1$ excited states of Hg I

K. Blagoev* and V. Pentchev
Institute of Solid State Physics, 72 Tzarigradsko Chausee, BG-1784 Sofia, Bulgaria

E. Biémont†
Astrophysique et Spectroscopie, Université de Mons-Hainaut, 15 Rue de la Halle, B-7000 Mons, Belgium

Z. G. Zhang, C.-G. Wahlström, and S. Svanberg
Department of Physics, Lund Institute of Technology, P.O. Box 118, S-221 00 Lund, Sweden
(Received 18 January 2002; revised manuscript received 1 July 2002; published 27 September 2002)

Natural radiative lifetimes have been measured along the $6sns\ ^3S_1$ ($n=7-10$) and $6snd\ ^3D_1$ ($n=6-11$) Rydberg series of neutral mercury using time-resolved laser-induced fluorescence spectroscopy in a laser-produced mercury plasma. The states of Hg I investigated in the present work were populated from the ground state by a stepwise excitation process. Relativistic Hartree-Fock calculations, including intravalence interactions and core-polarization effects, have been performed and the theoretical lifetimes have been compared with the measurements.

DOI: 10.1103/PhysRevA.66.032509 PACS number(s): 32.70.Cs, 42.62.Fi

I. INTRODUCTION

The first spectrum of mercury has attracted the attention of many investigators. As a result more than 250 energy levels are quoted in the Natl. Bur. Stand. (U.S.) compilation by Moore [1]. The ground level is $[Kr]4d^{10}\ 4f^{14}\ 5s^2\ 5p^6\ 5d^{10}\ 6s^2\ ^1S_0$. The Rydberg series $6snl$ have been observed up to rather high n (principal quantum number) values (i.e., $25s$, $26p$, $29d$, and $15f$). The $np\ ^3P$ levels were investigated for $n=18-60$ [2]. Additional observed levels belong to the configurations $5d^{10}6p^2$, $5d^96s^2nl$ (with $nl=6p$ to $18p$, $5f$ to $9f$). Radiative lifetimes of the triplet $6snl\ ^3L$ excited states of Hg I have been the subject of experimental and theoretical investigations for a long time, but almost all the published papers were dedicated to the low-lying excited states, with $n=6-8$ (see below). This is due to the fact that the most intense spectral lines originate from these three low-lying states, which have been investigated in detail using different experimental methods. It is important, however, to measure the radiative constants along the spectral series for higher ($n>8$) Rydberg states because the populations of the upper excited states determine the total emission in different mercury light sources. It is also interesting to investigate the radiative parameters along the spectral series in order to find out whether the intensity of the emitted radiation is influenced or not by perturbations.

These considerations apply to a full extent to the $6sns\ ^3S_1$ states. The radiative lifetime of the $6s7s\ ^3S_1$ state (from which the well-known blue-green $6s6p\ ^3P°$-$6s7s\ ^3S_1$ triplet originates) has been thoroughly investigated. Moreover, the strong lines involving the $6s7s\ ^3S_1$ level give the possibility to perform photon-photon coincidence cascade-free experiments [3–5]. The same excited state was also investigated using the beam-foil method [6], the level-crossing technique [7], and the time-resolved method, with laser excitation [8,9] or with nonselective electron excitation [10]. The results obtained, however, differ considerably and the disagreements among the various sets of data for this state are manifest both in old papers and in recent ones. For the $6s8s\ ^3S_1$ level, the radiative lifetime was obtained by the beam-foil technique [6] and the time-resolved approach using either laser [8] or pulsed electron excitation [10]. The results of the latter two experiments agree well. For $6s9s\ ^3S_1$, there is only one result published and it was obtained by the pulsed electron delayed-coincidence method [10].

The radiative lifetimes of the $6snd\ ^3D$ series of Hg I were also investigated but, as is the case for other spectral series, the analyses were frequently restricted to the low lying states having principal quantum numbers $n=6$ and 7. For the $6snd\ ^3D_2$ series, the most detailed investigation was extended up to $n=11$ [11], these excited states being reached by two-photon excitation from the ground state $6s^2\ ^1S_0$. The $6snd\ ^3D_{1,3}$ ($n=6,7$) excited levels were investigated by the beam-foil method [6,12], by the time-resolved approach using laser excitation from the metastable $6s6p\ ^3P_1°$ level [8], and by a stepwise excitation, where the first step was electron excitation of the resonance $6s6p\ ^1P_1°$ level while the second step was performed by laser excitation [13]. The level crossing technique was also employed to measure the lifetimes of the $6s6d\ ^3D_{1,2,3}$ levels [14,15].

Most of the theoretical works devoted to the study of the radiative properties of Hg I have concentrated on the low lying levels, particularly $6s6p\ ^{1,3}P_1°$. The resonance transition of Hg I has been the subject of different investigations because it was found early (see, e.g., Shorer [16]) that core polarization effects (CP) had a substantial influence on the oscillator strength of this transition, reducing the frozen-core or "valence correlation only" f value by about 40%. As a consequence, the mercury atom has become a testing ground for model potentials attempting to describe accurately the interactions between the core and valence electrons of the

*Electronic address: kblagoev@issp.bas.bg
†Also at: IPNAS (Bâtiment B 15), Université de Liège, Sart Tilman, B-4000 Liège, Belgium.

atom. This has motivated further studies analyzing the importance of CP effects on this transition and on the intercombination line $6s^2\ ^1S_0$-$6s6p\ ^3P_1^\circ$ (see, e.g., Refs. [17–21]). More recently, the relativistic random-phase approximation has been applied with success for a treatment of core-polarization effects in Hg I with the result that the discrepancies between theoretical and experimental f values were considerably reduced [22,23]. In Ref. [15], the $6s7d\ ^3D$ states were studied both theoretically and experimentally. The oscillator strengths of the transitions $6s6p\ ^3P^\circ$-$6sns\ ^3S_1$ were calculated within the framework of the Coulomb approximation [24] and, from these data, the radiative lifetime of the $6s7s\ ^3S_1$ level was obtained. For higher $6sns\ ^3S_1$ levels, an upper limit of the radiative lifetimes could be obtained [24]. Among the most extensive theoretical analyses devoted to Hg I, let us mention Ref. [25] in which the radiative lifetimes of the $6sns\ ^{1,3}S$ ($n=7$–9), $6snd\ ^{1,3}D$ ($n=6$–9), and $6snp\ ^{1,3}P^\circ$ ($n=6$–8) terms were calculated using a model potential method. The transitions $6s^2\ ^1S_0$-$6snp\ ^1P_1^\circ$, $^3P_1^\circ$ have also been extensively considered by Migdalek and Baylis [19] up to $n=20$ in the framework of a relativistic intermediate coupling self-consistent-field approximation, but the fact that correlation effects were considered in the calculations in a simplified way limits the scope of the results.

In the present work, we have carried out natural radiative lifetime measurements of the $6sns\ ^3S_1$ ($n=7$–10) and $6snd\ ^3D_1$ ($n=6$–11) levels in Hg I using a two-step excitation time-resolved laser-induced fluorescence technique. In addition, calculations were performed with the relativistic Hartree-Fock (RHF) approach considering configuration interaction among the outer electrons and also including core-polarization effects. This method has been applied with success, recently, in the case of a neutral heavy element, Cd I, and along its isoelectronic sequence [26], and has appeared in excellent agreement with the fully relativistic multiconfiguration Dirac-Fock method taking the valence and core-valence correlation effects into account.

The dependence of the radiative lifetimes of both spectral series upon effective principal quantum number was considered and its relation with the quantum defect dependence was analyzed.

II. EXPERIMENTAL SETUP

In the present experiment, the lifetimes of ten Hg I Rydberg levels, belonging to two different series, i.e., $6sns\ ^3S_1$ ($n=7$–10) and $6snd\ ^3D_1$ ($n=6$–11), were measured using a two-step excitation time-resolved laser-induced fluorescence technique. A simplified energy level scheme relevant to the present experiment is shown in Fig. 1. The experimental schemes considered in the measurements are summarized in Table I.

The experimental setup used in the experiment is shown in Fig. 2. Free Hg atoms were obtained by laser ablation. A solid target of HgS, rotating in a vacuum chamber, was irradiated perpendicularly by a focused Nd:YAG laser (A) (Continuum Surelite), characterized by a 532 nm wavelength, a 10 Hz repetition rate, and a 10 ns pulse duration. The pulse,

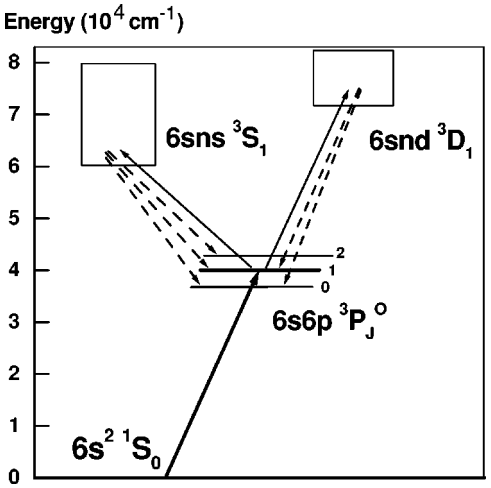

FIG. 1. A simplified energy level diagram of Hg I with relevant excitation scheme.

applied with a variable energy (0.5–1.5 mJ), caused an expanding plasma, rising into the interaction zone about 10 mm above the target, where the center of the vacuum chamber is located. Some time after the ions in the plasma have left the interaction zone, the neutral Hg atoms arrived, the ions moving much faster than the neutrals. In order to excite the Hg atoms, a Ti:sapphire laser, pumped by a Nd:YAG laser (B) (Continuum NY-82) with 8 ns pulse width and 400 mJ pulse energy, was frequency-tripled using a nonlinear optical system including a KDP crystal, a retarding plate, and a BBO crystal. The third harmonic from the system was selected using a quartz Pellin-Broca prism and sent into the interaction zone horizontally, exciting the Hg atoms from the ground state $6s^2\ ^1S_0$ to the level $6s6p\ ^3P_1^\circ$ using the 253.73 nm transition. In order to excite the atoms from the $6s6p\ ^3P_1^\circ$ to the levels studied, 8 ns pulses emitted by another Nd:YAG laser (C) (Continuum NY-82 injection seeded) were sent to a stimulated Brillouin scattering (SBS) compressor to shorten the pulses. The pulse duration of the output from the SBS compressor was about 1 ns [27]. These compressed pulses were used to pump a dye laser (Continuum Nd-60). DCM, R610, R640, and R6G dyes were employed separately in order to have the tunable dye laser working in different wavelength ranges. The dye laser was frequency-doubled (2ν) in another KDP crystal. In most cases, Raman shifted components, obtained in a cell filled with hydrogen at 10 bars, were employed to excite the atoms to the states measured.

In the experiment, all three Nd:YAG lasers were triggered externally by two digital delay generators (Stanford Research System, Model 535) mutually connected, which enabled temporal synchronization of the two excitation lasers and also a free variation of the delay time between the ablation and excitation lasers. The fluorescence, due to the natural decay from the levels studied, was imaged by two lenses and concentrated on the entrance slit of a vacuum monochromator, and detected by a Hamamatsu R3809U-58 photomultiplier with a rise time of about 170 ps. The time-resolved signal was acquired and averaged using a digital transient

TABLE I. The levels measured and the corresponding excitation schemes.

Measured state	Upper level energy [a] (cm^{-1})	Lower level energy [a] (cm^{-1})	Excitation λ (vac.) (nm)	Excitation scheme [b]	Observation λ_{obs} (air) (nm)
$6s7s\ ^3S_1$	62350.456	39412.300	435.955	$2\ \nu_1 + 2S$	435.8
$6s8s\ ^3S_1$	73961.296	39412.300	297.186	$2\ \nu_2$	289.4
$6s9s\ ^3S_1$	78216.261	39412.300	257.706	$2\ \nu_2 + AS$	292.5
$6s10s\ ^3S_1$	80268.056	39412.300	244.764	$2\ \nu_1 + 2AS$	275.9
$6s6d\ ^3D_1$	71336.164	39412.300	312.245	$2\ \nu_1$	296.7
$6s7d\ ^3D_1$	77084.632	39412.300	265.447	$2\ \nu_3 + AS$	265.4
$6s8d\ ^3D_1$	79678.708	39412.300	248.346	$2\ \nu_1 + 2AS$	237.8
$6s9d\ ^3D_1$	81071.027	39412.300	240.046	$2\ \nu_3 + 2AS$	230.2
$6s10d\ ^3D_1$	81904.500	39412.300	235.337	$2\ \nu_2 + 2AS$	225.9
$6s11d\ ^3D_1$	82443.000	39412.300	232.392	$2\ \nu_2 + 2AS$	223.2

[a]From the energy levels by Moore [1].

[b]ν_1 means frequency of DCM dye laser, ν_2 means frequency of R6G dye laser, ν_3 means frequency of R610+R640 dye laser, AS means anti-Stokes component, *S* means Stokes component; 2 in the 2AS or 2S means the second-order, and 2ν means frequency-doubling.

recorder (Tektronix Model DSA 602), and then sent to a personal computer for lifetime evaluation.

III. MEASUREMENTS AND RESULTS

In order to obtain reliable experimental lifetime values, several steps were taken to check for possible sources of errors and to avoid the influence of unwanted physical effects on the measurements. It was verified, for all the levels measured, that the correct level was excited by tuning the monochromator to check the different possible decay branches, and, in each case, the strongest branch was used for observing the fluorescence decay. A magnetic field, provided by a pair of Helmholtz coils, was applied to verify that Zeeman quantum beats do not influence our experiments because of the largely unpolarized detection scheme (the grating can cause some polarization).

In the measurements, long delay times between the ablation and excitation laser, 20–40 ms, were adopted to eliminate possible flight-out-of-view effects. The adopted long delay time implies that the speed of the observed moving atoms was several hundred meters per second. The longest lifetime value measured in the experiment is only about 150 ns. Thus, it is enough, in order to avoid the flight-out-of-view effects, to adopt for the slit of the monochromator a width of about 3 mm. To make sure that the experimental lifetimes were not affected by radiative trapping and collisions, the ablation pulse energy and the delay time were changed, which is equivalent to changing the atomic density.

For the acquirement of each decay curve, the excitation laser was kept weak enough to avoid errors due to a possibly nonlinear response of the detector. Therefore for each decay curve averaging data from 1000–4000 shots was needed in order to obtain a good signal-to-noise ratio. For two short-lived states, with lifetimes smaller than 10 ns, the lifetime of the recorded decay was evaluated by fitting the curve with a convolution between a detected laser pulse and an exponential function with adjustable parameters. For the other states, the lifetime of the curve was obtained by directly fitting the curve to an exponential. A typical experimental curve with the corresponding fit is shown in Fig. 3. For each state measured, more than ten time-resolved fluorescence decay curves were typically recorded under different experimental conditions. The evaluated lifetimes from these curves were found to coincide nicely. The final lifetime of each state was

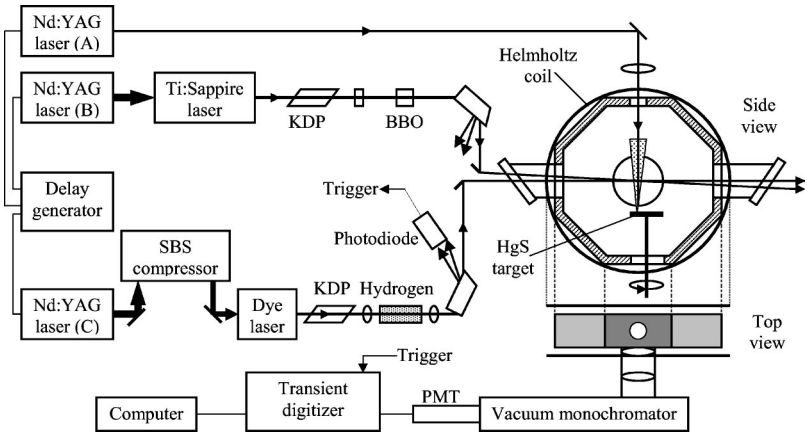

FIG. 2. Experimental setup.

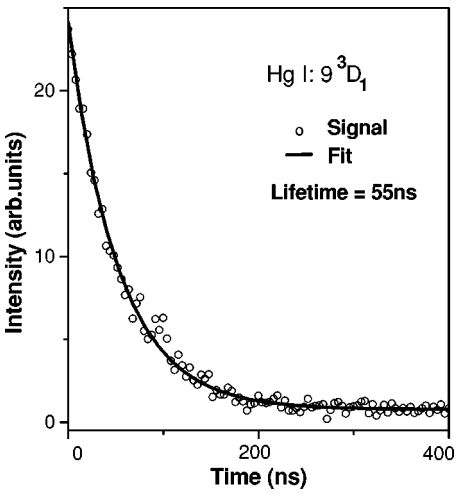

FIG. 3. A typical time-resolved fluorescence signal and an exponential fit.

formed by averaging these evaluated lifetimes. The lifetimes measured are reported in Table II, where the error bars reflect not only the statistical scattering, but also a conservative estimate of the possible remaining systematic errors.

IV. CALCULATIONS

For a heavy atomic system such as mercury, relativistic effects and also intravalence and core-valence interactions must be taken into account simultaneously for calculating the atomic structure. In practice, computer capabilities impose severe limitations on the number of interacting configurations which can be considered in the calculations. In the present case, the HFR method was used for the atomic structure calculations [28]. Cowan and Griffin [29] have shown that the contraction of valence orbitals due to relativistic effects can be mimicked in a nonrelativistic approach by adding to the Schrödinger Hamiltonian potentials containing mass-correction and Darwin terms. Migdalek and Baylis [30] as well as Migdalek and Marcinek [31] have suggested an approach (for a review, see also [32]) in which most of the intravalence correlation is represented within a configuration interaction scheme while core-valence correlation is described by a core-polarization model potential with a core-penetration corrective term. We have introduced these corrections in the RHF equations [28]. For that purpose, we added to the radial equations of the valence orbitals the one-particle potential:

$$V^{Pol}(r)=\frac{-\alpha_d r^2}{2(r^2+r_c^2)^3}, \tag{1}$$

where α_d is the static dipole polarizability of the ionic core and r_c is the cutoff radius. We corrected the nonequivalent electron part of the exchange potential between valence subshells by the two-particle term:

$$B_{i,j}^{Pol}=\frac{-\alpha_d r}{2(r^2+r_c^2)^{3/2}}\begin{pmatrix} l_i & 1 & l_j \\ 0 & 0 & 0 \end{pmatrix}^2 \times\left[\int_0^\infty \frac{r_2}{(r^2+r_c^2)^{3/2}}P_j(r_2)P_i(r_2)dr_2 + \int_0^{r_c}\frac{r_2}{r_c^3}P_j(r_2)P_i(r_2)dr_2\right], \tag{2}$$

where P_i and P_j are the radial parts of the atomic orbitals. The second part of Eq. (2) corresponds to the penetration of the core by the valence orbitals. The interaction between the modified electric fields experienced by the valence electrons is the first part of Eq. (2). The dipole-moment operator, $\vec{d}=-\vec{r}$, of the valence electron has to be replaced by

$$\vec{d}=-\vec{r}+\alpha_d\frac{\vec{r}}{(r^2+r_c^2)^{3/2}}+\alpha_d\frac{\vec{r}}{r_c^3}\mathrm{rect}(0,r_c), \tag{3}$$

where

$$\mathrm{rect}(0,r_c)=\begin{cases}1, & 0\leqslant r\leqslant r_c\\ 0, & r>r_c.\end{cases}$$

The third part of Eq. (3) is the penetration correction.

Two different RHF calculations (A and B) were performed in the present work using Cowan's code modified for the inclusion of CP effects.

In calculation A, the following configurations were retained (the core being $5d^{10}$): $6s^2$, $6sns$ ($n=7$–18), $6snd$ ($n=6$–18), $6p^2$, $6pnf$ ($n=5-10$), $6pnp$ ($n=7$–10), $6d^2$, $6dns$ ($n=7$–10), and $6dnd$ ($n=7$–10) (even parity) and $6snp$ ($n=6$–18), $6snf$ ($n=5$–18), $6pns$ ($n=7$–10), $6pnd$ ($n=6$–10), $6dnp$ ($n=7$–10), and $6dnf$ ($n=5$–10) (odd parity). This set of 92 configurations includes only valence - valence correlations. Core-valence interactions were included in the model through the use of the CP formulas hereabove described and applied with success in a recent past for different complex atomic systems belonging to lanthanide ions (see, e.g., La III - Lu III [33], Er III [34], Pr III [35,36], Tm III [37], and Yb III [38]). The approach followed is similar to that adopted in previous works [17–21,39] concerning the same atom (Hg I). The CP parameters were chosen equal to $\alpha_d=8.098a_0^3$ and $r_c=1.449a_0$. These values correspond to the static dipole polarizability of the ionic core Hg III as computed by Fraga *et al.* [40] and to the expectation value of r for the outermost core-orbitals ($5d^{10}$) as calculated by Migdalek and Baylis [17]. The adopted value for α_d is close to the value derived from experiment (i.e., $\alpha_d = 8.40$ a_0^3 according to [40–42]). The theoretical lifetime values are given in column 3 of Table II where they are compared with the experimental results as obtained in the present work (see the second column of the same table). Although the agreement is satisfying for the D states, larger discrepancies are observed for the S states. For the Rydberg levels $6sns$ and for the first member of the series $6snd$, the RHF values are smaller than the experimental results indicating that the po-

TABLE II. Observed and calculated lifetimes and comparison with previous results.

State	$\tau_{\text{this work}}$(ns)			$\tau_{\text{previous work}}$(ns)	
	Exp.	Calc.		Exp.	Calc.
		A	B		
$6s7s\ ^3S_1$	8.0(7)	7.4	6.2	7.7(4) [a], 8.4(4) [b], 8.2(2) [c], 8.2(5) [d], 8.0(4) [e], 8.1(5) [f], 10.5(5) [g], 11(2) [h]	9.6 [m], 8.4 [n]
$6s8s\ ^3S_1$	24.2(25)	20	18	14.0(15) [d], 22.1(11) [e], 22.5(10) [g]	21 [n]
$6s9s\ ^3S_1$	53(3)	22	36	47.7(15) [g]	39 [n]
6s10s $^3S_1$	92(7)	52	62		
$6s6d\ ^3D_1$	6.8(6)	5.6	4.6	6.2(6) [d], 6.0(6) [i], 7.2(4) [j], 6.2(3) [k]	6.9 [n]
$6s7d\ ^3D_1$	17(1.5)	14	13	12.4(5) [l]	10.4 [l], 16 [n]
$6s8d\ ^3D_1$	32(2)	32	28		
$6s9d\ ^3D_1$	56(3)	48	53		
$6s10d\ ^3D_1$	84(5)	88	92		
$6s11d\ ^3D_1$	93(9)	165	149		

[a]Photon-photon coincidence method [3].
[b]Photon-photon coincidence method [4].
[c]Photon-photon coincidence method [5].
[d]Beam-foil method [6].
[e]Laser excitation from the $6s6p\ ^3P$ states [8].
[f]Delayed-coincidence method; laser excitation from the $6s6p\ ^3P_1$ state [9].
[g]Delayed-coincidence method; pulsed electron excitation [10].
[h]Level-crossing method [7].
[i]Beam-foil method [12].
[j]Delayed-coincidence method; laser excitation from the $6s6p\ ^1P_1$ state [13].
[k]Level-crossing method [14].
[l]Level-crossing method, theory: Coulomb approximation [15].
[m]Theory: Coulomb approximation [24].
[n]Theory: model potential method [25].

larization effects could have been underestimated. Using $\alpha_d = 8.40a_0^3$ instead of $\alpha_d = 8.098a_0^3$ would modify (i.e., increase) the lifetime values by less than 1%. In order to take into account the interactions with the distant configurations not introduced explicitly in the model, it is a common practice [28] to introduce some scaling factors for the Slater integrals, spin-orbit, or configuration interaction integrals. The effect of this procedure was tested: considering a scaling factor of 0.85 would lead to a mean increase of the lifetime values by about 6% for the $6sns\ ^3S_1$ levels and to a modification by less than 4% (decrease or increase) for the $6snd\ ^3D_1$ levels.

To further test the sensitivity of the calculations, an additional more elaborate calculation was performed. In calculation B, the effect of opening the $5d^{10}$ core was considered. Concretely, the following configurations were retained in the calculations: $5d^{10}6s^2$, $5d^{10}6sns$ $(n=7-15)$, $5d^{10}6snd$ $(n=6-15)$, $5d^{10}6p^2$, $5d^{10}6pnp$ $(n=7-9)$, $5d^{10}6d^2$, $5d^{10}6dns$ $(n=7-9)$, $5d^{10}6dnd$ $(n=7-9)$, $5d^96s7s^2$, $5d^96s^27s$, $5d^96s^28s$, $5d^96s6d^2$, $5d^96s^2nd$ $(n=6-8)$, $5d^96p^2ns$ $(n=6-8)$, and $5d^96p^2nd$, $(n=6-8)$ for the even configurations and $5d^{10}6snp$ $(n=6-15)$, $5d^{10}6snf$ $(n=6-15)$, $5d^{10}6pns$ $(n=7-9)$, $5d^{10}6pnd$ $(n=6-9)$, $5d^{10}6dnp$ $(n=7-9)$, $5d^{10}6dnf$ $(n=5-9)$, $5d^96s^2np$ $(n=6-8)$, $5d^96s^2nf$ $(n=5-8)$, and $5d^96p^2np$ $(n=7$ to $8)$ for the odd configurations, the Rydberg series being limited to $n=15$ basically for computer reasons (large energy matrices). In the latter model, the CP parameters were chosen equal to $\alpha_d = 5.804a_0^3$ and $r_c = 1.372a_0$. These values correspond to the dipole polarizability of the ionic core Hg IV as computed by Fraga *et al.* [40] and to the expectation value of r for the outermost core-orbitals $(5d^9)$ as calculated by the RHF technique, respectively. The corresponding lifetimes are compared (column 4 of Table II) to the experimental measurements (column 2 of Table II) of the present work. For most of the levels, the agreement with experiment is improved compared to calculation A, the improvement resulting from a better representation of the CP effects. These results were obtained without the introduction of any scaling factor for the radial integral. Considering the same scaling factor as in the previous calculation (85%) would lead to a change of typically a few percent (<10) for most of the lifetimes, larger changes being induced for the odd parity levels as it was the case in calculation A.

The persistent discrepancies theory - experiment observed for the higher Rydberg states along the two series and the fact that they are increasing with n indicate probably that a more realistic theoretical model including many additional high-n configurations would be needed. The consideration of such a model, in the present work, was prevented basically by the available computer capabilities.

V. DISCUSSION AND COMPARISON WITH PREVIOUS RESULTS

Previous experimental and theoretical results are presented in columns 5 and 6 of Table II, where it can be seen that the radiative lifetime of the $6s7s\ ^3S_1$ state obtained in the present work agrees well with other authors' results derived by the beam-foil method [6], by a photon-photon coincidence method [3–5], and by a laser-excitation delayed coincidence method [8,9]. The larger values obtained in [10] as well as in [7] may be related to the influence of radiation trapping of the spectral lines in the case of the blue-green triplet, which has large transition probabilities and which connects the $6s7s\ ^3S_1$ state to the highly populated $6s6p\ ^3P^\circ$ levels. As was pointed out in [9], at a density of

10^{11} atoms/cm^3, the lifetime of the $6s7s\ ^3S_1$ state could be increased by 7%. Our experimental result for the $6s8s\ ^3S_1$ level is in agreement, within the errors, with those obtained by the delayed-coincidence method with pulsed electron excitation [10] or laser excitation [8]. The result for this level, obtained by beam-foil [6], is considerably smaller than other authors' results including our data.

Our lifetime for the $6s6d\ ^3D_1$ level agrees rather well with data obtained by beam-foil spectroscopy [6,12], by the delayed-coincidence method with stepwise excitation [13], and by the level-crossing method [14].

The present result for the $6s7d\ ^3D_1$ level is larger than the value obtained by the level-crossing method [15]. Our result agrees with values for the other $7d\ ^3D_{2,3}$ levels (measured in the mentioned work) if we consider that in the multiplets the radiative lifetimes of the levels usually have close values [8,11]. As it is well known, the radiative lifetimes of the excited states belonging to one spectral series are expected to follow a regular dependence versus the effective principal quantum number $n^*(n^*=n-\mu$, where μ is the quantum defect). For the spectral series where a one-electron approximation is adequate, this dependence is expressed by $\tau=\tau_0(n^*)^\alpha$, where τ_0 and α are coefficients characteristic of a spectral series. In particular, for the hydrogenic case, α has to be equal to 3. The data for the $6snd\ ^3D_{1,2}$ levels obtained in the present work allow one to consider this dependence.

In Fig. 4(a) a plot of $6snd\ ^3D_1$ level radiative lifetimes versus the effective principal quantum number n^* is presented on a ln-ln scale. In the same figure, the dependence of the quantum defect μ is also presented. The behavior of the two quantities, in an unperturbed system, is expected to be similar. The radiative lifetime dependence for the $6snd\ ^3D_1$ series is linear for the first members, but deviates from a straight line for $n=10$, 11. This dependence is similar to the $6snd\ ^3D_2$ dependence, which is presented in Fig. 4(b). In both cases, however, the quantum defect dependence has only small deviations from the linear one in the region $n=10$ to 11.

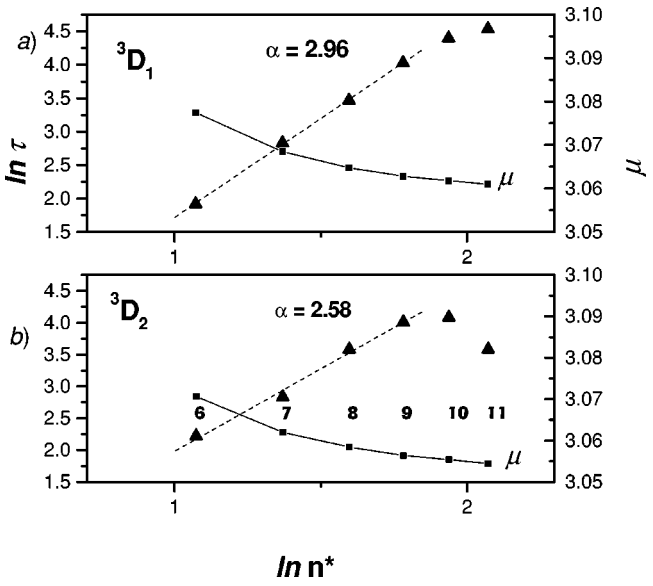

FIG. 4. Plots of the radiative lifetimes of $6snd\ ^3D_{1,2}$ ($n=6-11$) levels versus the effective principal quantum number and the dependence of the quantum defect μ for those series.

VI. CONCLUSIONS

In the present paper, radiative lifetimes of $6sns\ ^3S_1$ ($n=7-10$) and $6snd\ ^3D_1$ ($n=6-11$) excited states of Hg I have been measured. Stepwise laser excitation and laser induced fluorescence observations have been used in the experiment. The $\tau(n^*)$ dependence of the $6sns\ ^3S_1$ series is not perturbed, and is in agreement with the quantum defect dependence. The $\tau(n^*)$ dependence of the $6snd\ ^3D_{1,2}$ series, however, shows some deviations from the quantum defect curves for the quantum numbers $n=10$, 11.

The agreement between the laser lifetimes and the theoretical RHF values, as obtained in the present work, is satisfying for the $nd\ ^3D$ states (except for the n = 11 member along the Rydberg series) but larger discrepancies are observed for the ns ^{3}S states, particularly for the higher members of the sequence. A more realistic model, including many additional high excitation configurations, would probably be needed to reduce the discrepancies but this approach was prevented by the capabilities of the computer used. The present work indicates consequently some limitations to the use of the RHF approach for high members of the Rydberg series in heavy neutral atoms where a huge number of interacting configurations has to be considered.

A table with oscillator strengths (log gf) and transition probabilities (gA) of the lines depopulating the levels measured in the present work is available upon request.

ACKNOWLEDGMENTS

This work was supported by the European Community, under the Program ''Access to Research Infrastructures,'' Contract No. HPRI - CT 1999 - 00041. Some of us (E.B., K.B., and V.P.) are grateful to the colleagues from the Lund Laser Center for their kind hospitality and support. E.B. is grateful for support from the FNRS.

[1] C.E. Moore, *Atomic Energy Levels*, Vol. 3, NSRDS-NBS 3 (U.S. Government Printing Office, Washington, DC, 1971).
[2] A.T. Torsunov, N.B. Eshkobilov, and A.T. Halmanov, Opt. Spektrosk. **68**, 507 (1990).
[3] K.M. Mohamed, J. Quant. Spectrosc. Radiat. Transf. **30**, 225 (1983).
[4] C. Camhy-Val, A.M. Dumont, M. Dreux, and R. Vitry, Phys. Lett. **32A**, 233 (1970).
[5] R.A. Hold and F.M. Pipkin, Phys. Rev. A **9**, 581 (1974).
[6] T. Andersen and G. Sorensen, J. Quant. Spectrosc. Radiat.

Transf. **13**, 369 (1973).
[7] E.A. Alipieva and E.N. Kotlikov, Opt. Spectrosc. (USSR) **45**, 833 (1978).
[8] E.C. Benck, J.E. Lawler, and J.T. Dakin, J. Opt. Soc. Am. B **6**, 11 (1989).
[9] E.N. Borisov and A.L. Osherovich, Opt. Spectrosc. **50**, 631 (1981).
[10] A.L. Osherovich, E.N. Borisov, M.L. Burshtein, and Ya.F. Verolainen, Opt. Spectrosc. (USSR) **39**, 466 (1976).
[11] K. Blagoev, K. Iskra, and L. Windholz, Phys. Scr. **60**, 32 (1999).
[12] E.H. Pinnington, W. Ansbacher, J.A. Kernahan, T. Ahmad, and Z.Q. Ge, Can. J. Phys. **66**, 960 (1988).
[13] E.N. Borisov, A.L. Osherovich, and V.N. Yakovlev, Opt. Spectrosc. **47**, 193 (1979).
[14] Y. LeCluse, J. Phys. (France) **28**, 671 (1967).
[15] M. Chantepie, B. Laniepce, and J. Landais, Opt. Commun. **18**, 354 (1976).
[16] P. Shorer, Phys. Rev. A **24**, 667 (1981)
[17] J. Migdalek and W.E. Baylis, J. Phys. B **17**, L459 (1984).
[18] J. Migdalek and W.E. Baylis, J. Phys. B **17**, L459 (1984).
[19] J. Migdalek, and W.E. Baylis, J. Quant. Spectrosc. Radiat. Transf. **37**, 183 (1987).
[20] J. Migdalek and A. Bojara, J. Phys. B **20**, L1 (1987).
[21] J. Migdalek and A. Bojara, J. Phys. B **21**, 2221 (1988).
[22] H.-S. Chou and K.-N. Huang, Phys. Rev. A **45**, 1403 (1992).
[23] H.-S. Chou, H.-C. Chi, and K.-N. Huang, J. Phys. B **26**, 2303 (1993).
[24] P.F. Gruzdev, Opt. Spectrosc. **22**, 169 (1967).
[25] P. Hafner and W.H.E. Schwarz, J. Phys. B **11**, 2975 (1978).
[26] E. Biémont, C.F. Fischer, M.R. Godefroid, P. Palmeri, and P. Quinet, Phys. Rev. A **62**, 032512 (2000).
[27] Z.S. Li, J. Norin, A. Persson, C.-G. Wahlström, S. Svanberg, P.S. Doidge, and E. Biémont, Phys. Rev. A **60**, 198 (1999).
[28] R.D. Cowan, *The Theory of Atomic Structure and Spectra* (University of California Press, Berkeley, CA, 1981).
[29] R.D. Cowan and D.C. Griffin, J. Opt. Soc. Am. **66**, 1010 (1976).
[30] J. Migdalek and W.E. Baylis, J. Phys. B **11**, L497 (1978).
[31] J. Migdalek and R. Marcinek, J. Quant. Spectrosc. Radiat. Transf. **32**, 269 (1984).
[32] A. Hibbert, Phys. Scr. **39**, 574 (1989).
[33] E. Biémont, Z.S. Li, P. Palmeri, and P. Quinet, J. Phys. B **32**, 3409 (1999).
[34] E. Biémont, H.P. Garnir, T. Bastin, P. Palmeri, P. Quinet, Z.S. Li, Z.G. Zhang, V. Lokhnygin, and S. Svanberg, Mon. Not. R. Astron. Soc. **321**, 481 (2001).
[35] P. Palmeri, P. Quinet, Y. Frémat, J.-F. Wyart, and E. Biémont, Astrophys. J., Suppl. **129**, 367 (2000).
[36] E. Biémont, H.P. Garnir, P. Palmeri, P. Quinet, Z.S. Li, Z.G. Zhang, and S. Svanberg, Phys. Rev. A **64**, 022503 (2001).
[37] Z.S. Li, Z.G. Zhang, V. Lokhnygin, S. Svanberg, T. Bastin, E. Biémont, H.P. Garnir, P. Palmeri, and P. Quinet, J. Phys. B **34**, 1349 (2001).
[38] E. Biémont, H.P. Garnir, Z.S. Li, V. Lokhnygin, P. Palmeri, P. Quinet, S. Svanberg, J.-F. Wyart, and Z.G. Zhang, J. Phys. B **34**, 1869 (2001).
[39] M. Mohan and A. Hibbert, J. Phys. B **20**, 907 (1987).
[40] S. Fraga, J. Karwowski, and K. M. S. Saxena, *Handbook of Atomic Data* (Elsevier, Amsterdam, 1976).
[41] *Zahlenwerte und Funktionen aus Physik*, Landolt-Bornstein, Vol. 1 Atom-und Molekularphysik, Teil 1 Atome und Ionen (Springer, Berlin, 1950), pp. 399–404 .
[42] E.R. Mosburg, Jr., and M.D. Wilke, J. Quant. Spectrosc. Radiat. Transf. **19**, 69 (1978).